PII: S0032-3861(96)00678-7

Polymer Vol. 38 No. 7, pp. 1669–1676, 1997

0032-3861/97/$17.00 + 0.00

Computer simulation of the fracture of perfectly oriented polymer fibres

Tsunetoshi Matsuda* and Kazuo Tai
Research and Development Centre, UNITAKA Ltd, 23 Kozakura, Uji-shi, Kyoto 611, Japan
(Received 15 May 1996)

Fracture of perfectly oriented polymer fibres was studied by means of a computer simulation technique based on the ultimate structure model in order to estimate the upper limit of the tenacity of polymers with finite molecular weight. The fracture mechanism was also investigated in terms of average molecular weight and different nature of interchain interaction. It was observed that the tenacity of the model fibres increased with molecular weight and tended to approach the theoretical limit for the infinite molecular weight. In the cases of lower molecular weight, significant broadening of the stress distribution was observed under elevated stress, and the fracture behaviour was plastic. In the cases of higher molecular weight, the stress distribution was quite narrow until significant number of bond-cleavages occurred, and the fracture was brittle. The primary factor of fracture was found to be the chain-slippage in the lower molecular weight cases, and chain-scission in the higher molecular weight cases. Higher tenacity was marked when the polar interactions were introduced, especially in lower molecular weight cases. This can be attributed to the enhancement of chain binding by the polar interactions and suppression of chain-slippage.

(Keywords: computer simulation; theoretical tenacity of polymers; fracture)

INTRODUCTION

Ultimate values of the tenacity of various polymers, so-called theoretical tenacity, have often been quoted in designing high-performance polymer materials. The values were conventionally calculated from the strength of the chemical bond and the cross-sectional area of a polymer chain. Ito[1] calculated the theoretical tenacity of polyethylene to be 29.5 GPa. Other methods to estimate the theoretical tenacity of polymer fibres have also been proposed. Boudreaux[2] calculated the potential surface of a stretched polyethylene chain by the molecular orbital method and obtained the theoretical tenacity to be 19 GPa. Crist[3] considered a chain composed of segments connected by Morse function and analytically predicted the condition of chain scission. He concluded the tenacity of infinitely long chains should be one-third of that determined by the Morse function, which is about 10 GPa for polyethylene.

These theoretical works assume infinite molecular weight for the polymer. However, we can neither obtain such a polymer of infinite molecular weight nor make fibre with it. Therefore, it is useful for polymer modelling to estimate the upper limit of tenacity that we can reach with polymers of finite molecular weight. Termonia *et al.*[4–6] introduced the simulation model consisting of perfectly oriented polymer chains of finite length, and explained the structure–property relationship of highly oriented polyethylene fibres. Another factor affecting the tenacity is the characteristics of interchain interaction. Coulombic interaction and hydrogen bonding are especially important because they exist in many commercial polymers. The effect of the polar interactions has not been considered in the previous works on the theoretical tenacity[1–6] but must have an important role when the length of chains are finite. Therefore, we extended the model of Termonia *et al.* to include such polar interactions in this study.

The purpose of this work is first to estimate the upper limit of the tenacity of polymer fibres with finite molecular weight and next to discuss the fracture mechanism in terms of average molecular weight and the nature of interchain interaction.

METHODOLOGY

Models

In the model of Termonia *et al.*, the model fibre is composed of perfectly oriented polymer chains[4], where chains consist of covalently connected segments. All the chains were perfectly oriented to the fibre axis (z-axis) and aligned with regular separations in x and y directions. In other words, the initial structure of the model fibre is close to a single extended crystal containing point defects due to chain ends. The effect of molecular weight was evaluated by varying average chain length in the model. We formulated our model by introducing various modifications to the model of Termonia *et al.* One aspect of our interest is the effect of polar interactions among polymers on the ultimate tenacity. We took into account Coulombic interaction and hydrogen bond in addition to van der Waals interaction. Thus, we considered two models; (1) the nonpolar model in which only van der Waals interaction was taken into account as an interchain interaction and (2) the polar model in which Coulombic interaction and hydrogen bond were also introduced. Consequently, the nonpolar model represents the polymers in which polar

* To whom correspondence should be addressed

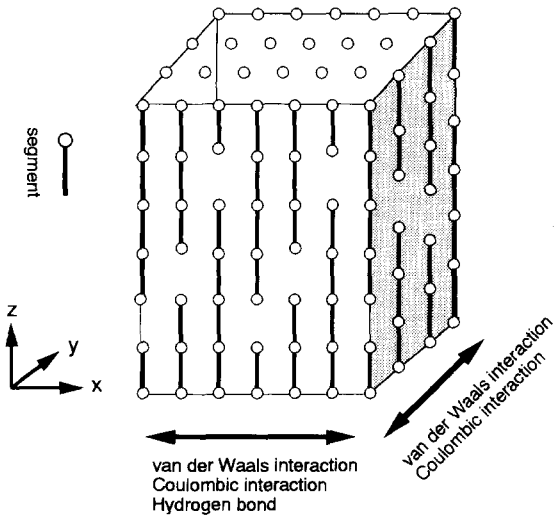

Figure 1 The schematic image of the model fibre

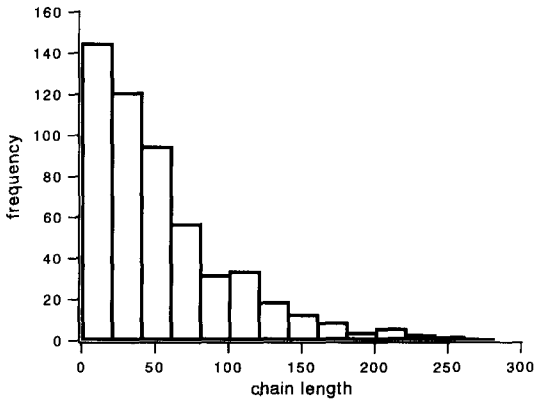

Figure 2 Distribution of chain length when the expected average chain length was 50 and total length of the fibre was 300

interaction is negligible such as polyethylene or polypropylene, and the polar model denotes the polymers in which Coulombic interaction and hydrogen bond exist such as polyamides. However, we used the same geometrical structure for both models for the simplicity of comparison. Since one of the typical polar polymers is nylon6, $(-NH(CH_2)_6CO-)_n$, we constructed a model referring the properties of nylon6 to this study. However, it should be noted that our model is not fully precise because various simplifications and modifications were introduced mainly to save the computation time.

The initial structure of the model fibre was constructed in the following way. First, we located segments on the rectangular lattice. Each segment represents a monomer unit of nylon6 ($NH(CH_2)_6CO$). Referring the unit cell of the α-form crystal of nylon6[7], we chose the lattice-spacing to be 4.8 Å, 4.0 Å and 8.6 Å, for x, y and z directions, respectively; the z direction is the fibre direction. In this sense Coulombic interaction is anisotropic for the x and y directions, and the hydrogen bond acts only for x direction. The schematic representation of the model fibre is shown in *Figure 1*. The number of lattice points was 200 or 300 for the z direction, and 10 for x and y directions, where periodic boundary condition was applied for x and y direction. Second, beginning with a segment at the bottom ($z = 0$) of the fibre, a chain was propagated toward the top of the fibre by connecting segments with a valence bond when a random number generated each time was larger than the probability for chain-termination, p_t, defined by

$$p_t = 1/P_0, \tag{1}$$

where P_0 denotes the average number of connected segments (average chain length) expected. This method gives the most probable distribution of chain length with a reaction degree P_0. In order to avoid the uncertainty of the effect of very short chains (less than three segments) and very long chains reaching both ends of the fibre, those cases were eliminated during the setup process of the system. As a result of this treatment, the average length of chains, P, obtained was somewhat different from the expected one, P_0, and fluctuates due to random processes. An example of the distribution of chain length is shown in *Figure 2*, here P_0 had been set to 50 and the resulting P was 55.

In order to cover a wide range of molecular weight, we considered a segment as several monomer units by multiplying an integer number, N_u, to each nonbonding interaction. This treatment was also introduced by Termonia *et al.*[4] and certified to work well. Since the molecular weight of a monomer of nylon6 is 113, the molecular weight for each case was obtained by multiplying 113 with $\bar{P}$. The cases we simulated are listed in *Table 1*.

Force fields

The potential of a bond, $U_b(l)$, was expressed by Morse function,

$$U_b(l) = D_b[1 - \exp\{-a(l - l_0)\}]$$
$$a = \left(\frac{k_b}{2D_b}\right)^{1/2} \tag{2}$$

Here, D_b is the bond energy, k_b is the initial force constant of the bond, l is the segment length, and l_0 is unstressed segment length, 8.6 Å (length of a monomer unit). We then obtain the force on a bond, $F_b(l)$, as a function of l,

$$F_b(l) = 2aD_b \exp\{-a(l - l_0)\}[1 - \exp\{-a(l - l_0)\}] \tag{3}$$

The maximum of force can be determined by the condition of

$$\frac{dF_b(l)}{dl} = 0 \tag{4}$$

Then, the bond length at the maximum force is

$$l_{max} = \ln 2/a + l_0 \tag{5}$$

The energy at the maximum force is given by

$$U_{b,max} = D_b/4 \tag{6}$$

The bond energy, D_b, has been reported 83.1 kcal mol^{-1} for a C-C bond and 69.7 kcal mol^{-1} for a C-N bond[8]. Since we consider a segment which mimics a monomer unit of nylon6, D_b is found to be 554.9 kcal mol^{-1} by summing up the bonding energy of five C-C bonds and two C-N bonds. Then, U_{max} is 138.7 kcal mol^{-1}. The force constant, k_b, was 85.9 kcal mol^{-1}Å^{-2}, converted from the experimental value for α-form crystal of nylon6 at low temperature, 270 GPa[9]. A bond cleaves when the

stress on it is elevated to certain degree. Zhurkov measured the rate of bond-cleavage in stressed fibres, and proposed the activated process[10]. Termonia *et al.* used Zhurkov's equation with different parameter sets in their simulation of highly oriented polyethylene fibres[4]. However, it should be noted that significant inhomogeneity of stress on bonds must exist in Zhurkov's experiment because he used real fibres which contain various structural inhomogeneities such as crystal, amorphous, etc. Therefore, force acting on the stress-concentrated bonds must be much higher than the applied bulk stress, and bond-cleavage can be over-estimated. Because we focus on the tenacity of upper limit then we can approach with polymers of finite molecular weight, we used the Morse function in judging bond-cleavage. We compared the energy of a bond, $U_b(l)$, calculated by equation (2) with the maximum bond energy, $U_{b,max}$ defined by equation (6). Then, the probability of bond cleavage, P_{break}, is given by

$$P_{break} = \tau \Delta t \exp\left\{\frac{U_{b,max} - U_b(l)}{kT}\right\} \quad (7)$$

where k is the Boltzman constant, and T is the temperature (in this study 300 K); τ was chosen to be 10^{11} as a typical frequency of a single bond: Δt is the time for an iteration of the simulation. The probability calculated by equation (7) exceeds unity when the bond strained more than 26%, and the stress at the time is about 28 GPa. This is the upper limit that the tenacity of our model reaches with infinite molecular weight and is identical to the conventionally used theoretical tenacity.

Non-bonding interactions were taken into account between adjacent chains. Evaluating van der Waals interaction among all atoms explicitly by any potential function such as Lennard-Jones 6–12 type function is impossible because of the enormous number of interactions. Termonia *et al.*[4] used a harmonic potential truncated at a small distance in order to describe van der Waals interaction among polyethylene chains, where force constant was chosen to be the shear modulus of polyethylene crystal. This may be a reasonable treatment while the strain is small. For larger strain, this assumption no longer has reality, and there is no absolute way to estimate van der Waals interaction explicitly. It may be possible to calculate the potential surface of a pair of short n-alkane chains by means of *ab initio* molecular orbitL (MO) methods using larger basis set. In this study, however, we employed a function having the same initial modulus with the shear of the polyethylene crystal and approaching smoothly zero at the separation in z direction to be l_0. The function we employed was

$$f_{vdw}(\Delta z) = k_s \Delta_z \left(1 - \frac{\Delta z}{l_0}\right)^n \quad (8)$$

where $f_{vdw}(\Delta z)$ is the force acting on two segments belonging to adjacent chains and separated by Δz for z direction. The value of force constant, k_s, was chosen to be 3.7 kcal mol^{-1} Å^{-2} converted from the shear modulus of polyethylene crystal, 3 GPa[4]. The factor n was arbitrarily chosen as 6, and hence the force assumed the maximum at $\Delta z - l_0/7$.

Coulombic interaction was calculated as between an oxygen and an aminoic hydrogen in a monomer unit by

$$U_c^0(R) = \frac{1}{4\pi\epsilon_0\epsilon}\frac{q_i^2}{R} \quad (9)$$

where charge q_i was chosen to be o.4 e.u., and R was calculated by

$$R^2 = \Delta z^2 + r_0^2 \quad (10)$$

where ϵ_0 is the dielectric constant of vacuum and r_0 is the closest distance between the hydrogen and the oxygen in the α-form crystal of nylon6. For chains adjacent in the zx plane, r_0 is 1.75 Å, and it is 4.0 Å for chains adjacent in yz plane. Dielectric constant of the system ϵ, was chosen to be 3.5. Coulombic interactions due to other atom-pairs were neglected because interactions among other atom-pairs are much smaller, and the interactions between same point-charges (oxygen–oxygen or hydrogen–hydrogen) may be reduced more effectively by the conformational change in a monomer. However, detailed discussion in atomic level is not our purpose in this study.

The most significant character of a molecule of nylon6 is its intermolecular hydrogen bond. We calculated the potential of hydrogen bond between segments belonging to different chains adjacent in zx plane by Dreiding type function[11]

$$U_{HB}(r_{DA}, \theta) = D_{HB}\left[5\left(\frac{r_{HB}}{r_{DA}}\right)^{12} - 6\left(\frac{r_{HB}}{r_{DA}}\right)^{10}\right]\cos^4\theta \quad (11)$$

We set D_{HB} to 4.0 kcal mol^{-1} and r_{HB} to 2.75 Å. r_{DA} is the distance between the hydrogen donor (N) and the acceptor (O).

All the interchain interactions described above were truncated at the distance when the separation in z direction was the unstressed segment length, $l_0 = 8.6$ Å, in order to save computation time. For the Coulombic interaction, the force acting 8.6 Å apart is still considerable and discontinuity of the force by sudden truncation causes severe instability of the stimulation. Therefore, we modified Coulombic interaction by

$$U_c(R) = U_c^0(R) - U_c^0(R_c) - \left(\frac{dU_c^0(R)}{dR}\right)_{R=R_c}(R - R_c) \quad (12)$$

where $U_c^0(R)$ is the original potential calculated by equation (9), and R_c is the cutoff distance.

Simulations

Our simulation was performed by calculating the equilibrium position of each segment along the fibre direction against the increasing strain, keeping the position perpendicular to the fibre direction unchanged. The model fibres were extended with small ratio (0.05%) at a time. This was done by simply multiplying 1.0005 to z coordinates of all segments except for ones at the bottom, where the z coordinates are always 0. The strain rate was chosen to be 120% min^{-1} which is comparable with the standard testing method for synthetic fibres[12]. The time for an iteration, Δt, should then be 0.025 s. After the expanding cycle, the positions of all the segments except for those at fibre ends were adjusted by minimization of potential. We employed the steepest decent algorithm for the potential minimization. Here, potential is not fully minimized at each iteration, because most of the adjustment of the segment positions by the

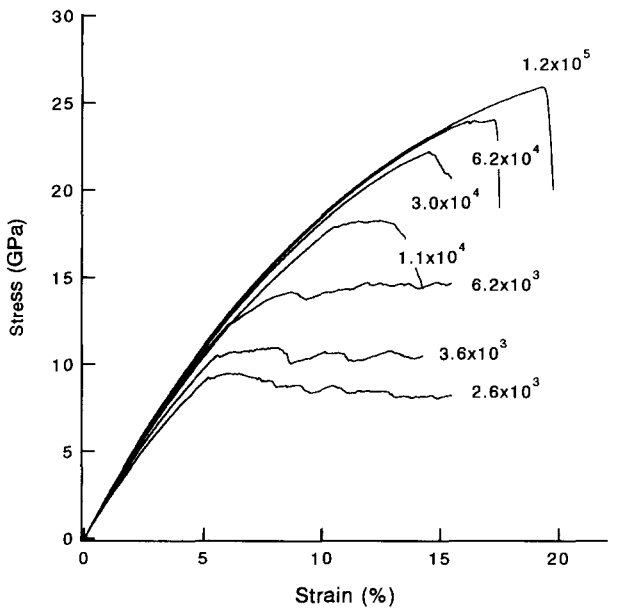

Figure 3 The stress–strain curves simulated for the nonpolar model fibres. Numbers on the curves are average molecular weight

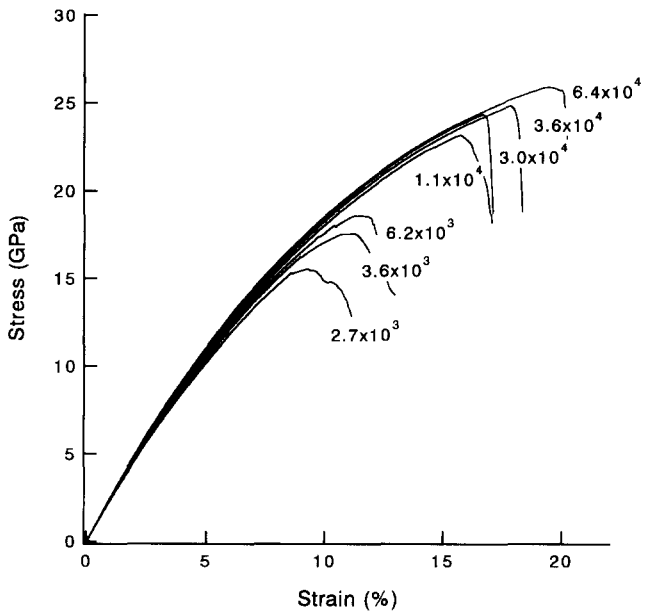

Figure 4 The stress–strain curves simulated for the polar model fibres. Numbers on the curves are average molecular weight

Table 1 Size and average chain length of the model fibres

Number of segments in z direction	P_0	Number of monomers united to a segment, N_u	Nonpolar model		Polar model	
			P	M_n	P	M_n
200	20	1	22	2.6×10^3	23	2.7×10^3
	30	1	31	3.6×10^3	31	3.6×10^3
	30	3	30	1.1×10^4	31	1.1×10^4
	30	10			31	3.6×10^4
300	50	1	53	6.2×10^3	53	6.2×10^3
	50	5	52	3.0×10^4	52	3.0×10^4
	50	10	53	6.2×10^4	55	6.4×10^4
	50	20	50	1.2×10^5		

minimization takes place in the first few steps, and great precision of the minimization is not only unnecessary for our purpose but also extremely time-consuming. We stopped the minimization at the maximum of 20 cycles.

After the minimization, the probability of bond-cleavage was calculated by the method described above, and compared with a random number between 0 and 1 generated each time. If the probability is larger than the random number, the bond cleaves. If any bond cleavage occurred, relaxations were performed again. The stress on the fibre is calculated based on the average stress on the segments in the fibre ends, and stress–strain data were restored. The fibres were extended at the constant strain rate until the total stress on the fibre exceeded the maximum which had been marked in the simulation, and the maximum were considered to be the tenacity of the fibre.

RESULTS AND DISCUSSION

Tensile properties

Simulated stress–strain (SS) curves for nonpolar models with various molecular weight are shown in *Figure 3*, here numbers on the curves are the molecular weight obtained by multiplying $113 N_u$ to the average chain length as described in the previous section (see *Table 1*). First, we look at the tenacity of the model fibres and the maxima of the curves. As molecular weight increases, the tenacity increases remarkably. A value of 26 GPa was achieved in the highest molecular weight case ($M_n = 1.2 \times 10^5$), which is very close to the upper limit of our model 28 GPa, to be expected for infinite molecular weight. Next, we discuss the profile of the curves. In all cases stress increases with strain up to some point (at a strain of 5%, 6%, 7%, 11%, 14%, 17%, and 19% in the cases of $M_n = 2.6 \times 10^3$, 3.6×10^3, 6.2×10^3, 1.1×10^3, 3.0×10^4, 6.2×10^4, and 1.2×10^5, respectively) where the slope of the curves discontinuously change. We call these points critical points in this study. The positions of the critical points shift toward higher stress and strain with an increasing molecular weight. All curves are similar to the profile of the Morse function before the critical points, and the deformation can be considered elastic in this region. However, the slopes of the curves, the moduli of the model fibres, are noticeably different. The slopes of the curves are smaller in the lower molecular weight cases and become larger with increasing molecular weight. Those in the highest molecular weight cases ($M_n \geqslant 6.2 \times 10^4$) are almost identical to the one defined by the Morse function. The reason for small

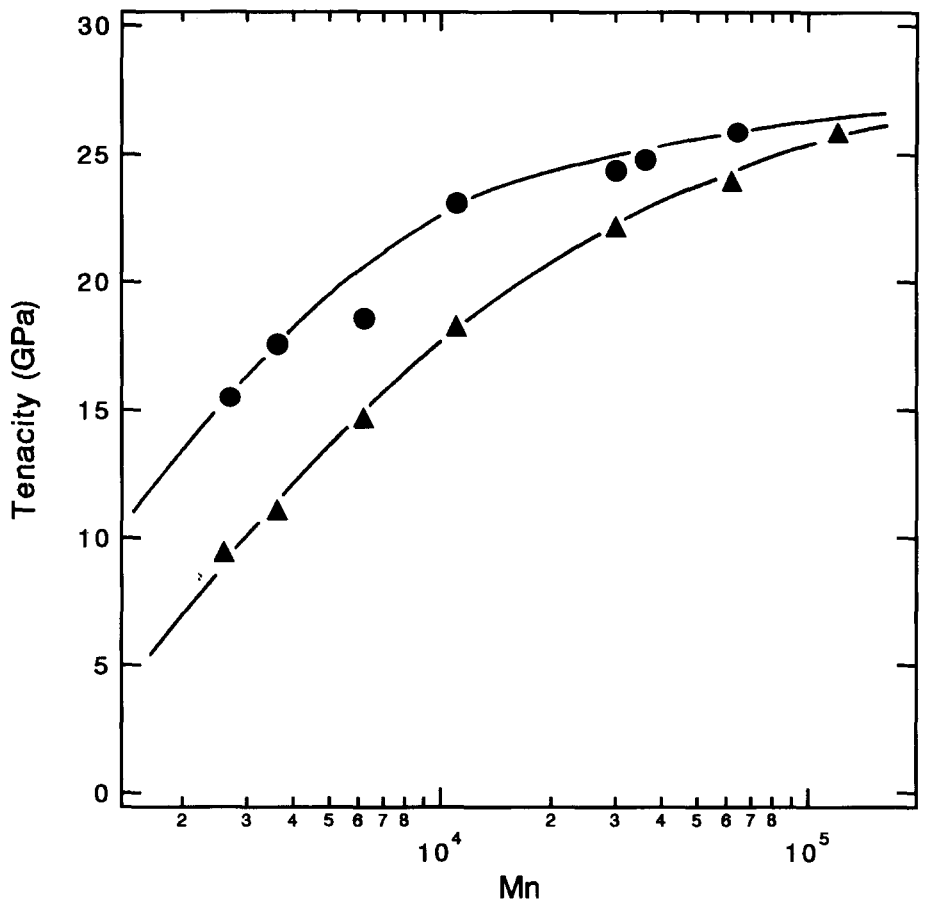

Figure 5 Molecular weight dependence of the tenacity of nonpolar (▲) and polar (●) model fibres

moduli in the lower molecular weight cases will be discussed later. The behaviour of the curves after the critical points is significantly different. Plastic deformation was observed in the lower molecular weight cases ($M_n \leqslant 1.1 \times 10^4$), where the maxima of the curves and the critical points are not the same. Conversely, in the higher molecular weight cases ($M_n \geqslant 3.0 \times 10^4$), the stress suddenly falls after the critical points. Here, the critical points and the maxima are identical. We call the deformation behaviour observed in lower molecular weight cases *elastic–plastic* and the behaviours observed in higher molecular weight cases *elastic–brittle*. Since the profile of the curves before the critical points are similar to the Morse function in all cases, the deformation of the fibres can be described mainly by the elongation of bonds in this region. Therefore, the deformation before the critical point is quite elastic for every case. However, it was suggested that the deformation (or the fracture) mechanisms after the critical point must be completely different in cases of different molecular weights.

The SS curves for polar models are shown in *Figure 4*. The trend of the curves is similar to that observed in nonpolar models. The critical points were observed at about 8%, 9%, 11%, 16%, 17%, 18%, and 19% in the cases of $M_n = 2.7 \times 10^3$, 3.6×10^3, 6.2×10^3, 1.1×10^4, 3.0×10^4, 3.6×10^4, and 6.4×10^4, respectively. Apparently, the critical points are located at higher strain and stress than those observed in nonpolar model. Also, the tenacity is greater than that of nonpolar models with comparable molecular weight cases. In the lower molecular weight cases ($M_n \leqslant 6.2 \times 10^3$), the stress gradually decreases with strain after the critical points (not staying constant as observed in nonpolar models). This difference can be explained by the character of hydrogen bonds, which is strong but active only within a small distance. However, the gradual decrease of stress supports the plastic deformation. The trend of deformations in the lower molecular weight cases are elastic before the critical point and changes to plastic after it (elastic–plastic). In contrast, in the higher molecular weight cases ($M_n \geqslant 1.1 \times 10^4$) the stress suddenly drops at the critical point (elastic–brittle), and the critical points and maxima are the same. The molecular weight at which deformation pattern changes from elastic–plastic to elastic–brittle can be estimated to be $M_n \approx 3.0 \times 10^4$ in the nonpolar model and $M_n \approx 1.1 \times 10^4$ in the polar model. The slopes of the curves also depend on the molecular weight, but the reduction at the lower molecular weight cases is less than that in the nonpolar model.

The molecular weight dependence of the tenacity in two models is shown in *Figure 5*. One can see strong dependence of the tenacity on the molecular weight, but no simple power law was obtained in both models. It is obvious that the tenacity of polar models is considerably higher than that of nonpolar models, and the difference is more significant in the lower molecular weight region, while the difference becomes smaller in the higher molecular weight region. Two curves appear to meet for infinite molecular weight, where 28 GPa should be expected by the requirement of the model.

Fracture mechanism

In the previous section, different deformation behaviour was observed for the lower molecular weight cases

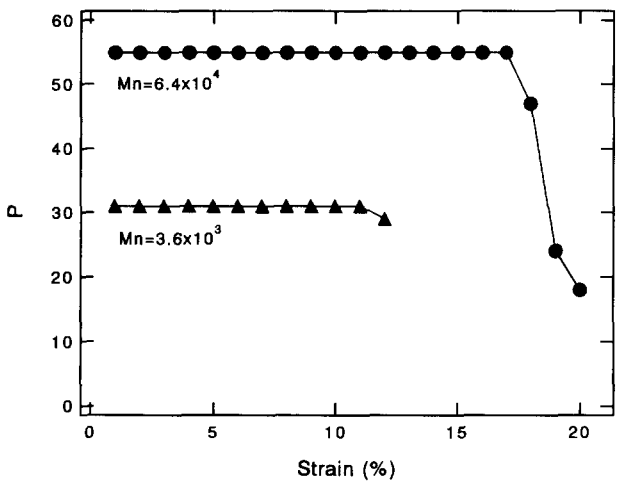

Figure 6 Change in the average chain length observed in polar model fibres with $M_n = 3.6 \times 10^3$ (▲) and $M_n = 6.4 \times 10^4$ (●)

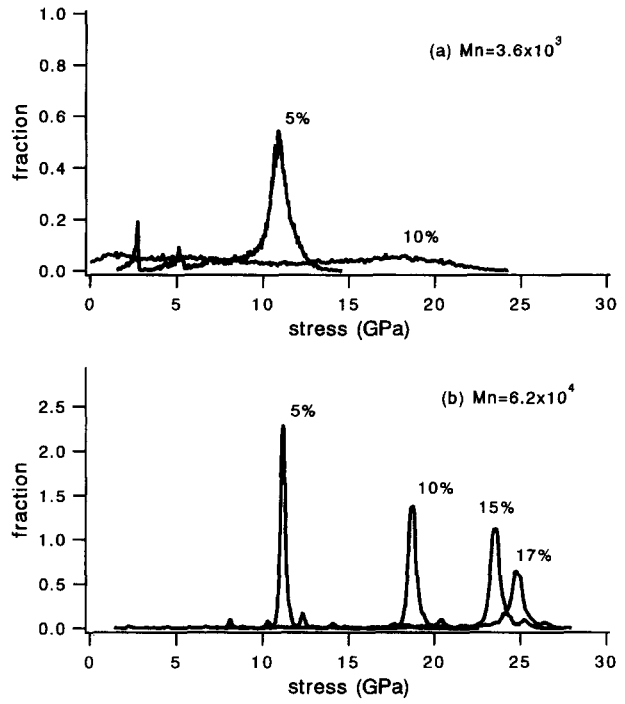

Figure 7 Distribution of stress on bonds observed in nonpolar model fibres with (a) $M_n = 3.6 \times 10^3$ and (b) $M_n = 6.2 \times 10^4$. Numbers are the strain at which the distribution was calculated

(elastic–plastic) and the higher molecular weight cases (elastic–brittle). In the following session we discuss the difference of the fracture mechanism as a function of molecular weight.

First, we calculated the degree of bond-cleavage during the simulations. We chose $M_n = 3.6 \times 10^3$ as the low molecular weight case and $M_n = 6.4 \times 10^4$ as the high molecular weight case of polar model, and the change in the average chain length in both cases are shown in *Figure 6*. Note that the interchain interaction per a segment is different in each model, as mentioned in the previous section (see *Table 1*). In the low molecular weight case, the average chain length did not change until a strain of 11% and slightly drops at 12%. Since the critical point observed in *Figure 4* was at a strain of about 9%, the transition of the deformation mode from elastic to plastic is not due to the chain-scission. In the high molecular weight case a remarkable drop in average chain length was first observed at a strain of 18%, and rapidly decreased for the higher strain. The maximum stress was pronounced at 19.5% (*Figure 4*), where the average chain length was less than half of the initial value. This indicates that the fracture was the result of an enormous number of bond-cleavages in the entire region of the fibre. The same tendency was observed in the simulations of the nonpolar model.

We then investigated the distribution of stress. *Figure 7* shows the distribution on the bonds calculated for the nonpolar models in the case of (a) $M_n = 3.6 \times 10^3$, as the low molecular weight, at strains of 5% and 10% and (b) $M_n = 6.2 \times 10^4$, as the high molecular weight, at strains of 5%, 10%, 15%, and 17%. At a strain of 5% the distribution in the low molecular weight case is considerably wider than that of the high molecular weight case. At a strain of 10% significant broadening was observed, indicating the great extent of stress concentration. Conversely, in the high molecular weight case the distribution is quite narrow until 15% and slightly broadened at the strain of 17% which is just below the fibre-breakage. It can be said that the deformation is highly homogeneous until very close to the fracture in high molecular weight case, and it must be the major reason for the very high tenacity. The distribution of the stress in polar models were also calculated and shown in *Figure 8*. The general trend is same as in the nonpolar model, and the peak positions at the same strain ratio are exactly the same. However,the distribution observed in the polar model was narrower than that in the nonpolar model. This must be the result of enhancement of interchain interaction by polar

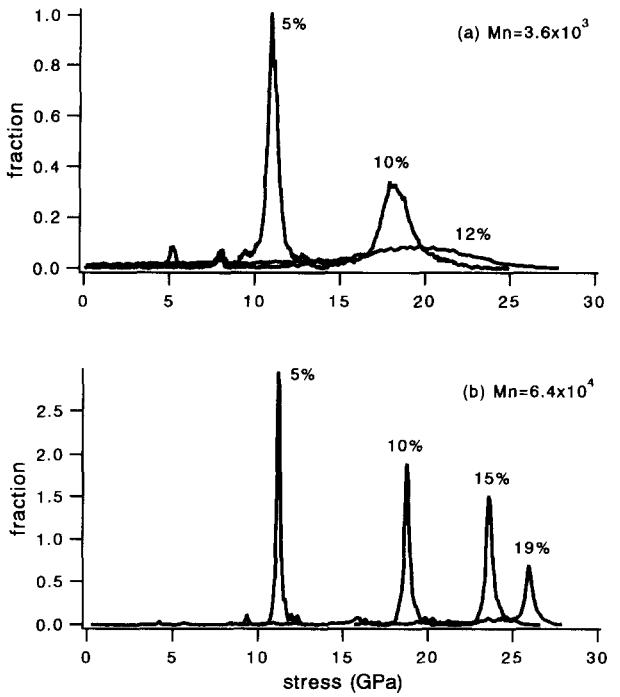

Figure 8 Distribution of stress on bonds observed in polar model fibres with (a) $M_n = 3.6 \times 10^3$ and (b) $M_n = 6.4 \times 10^4$. Numbers are the strain at which the distribution was calculated

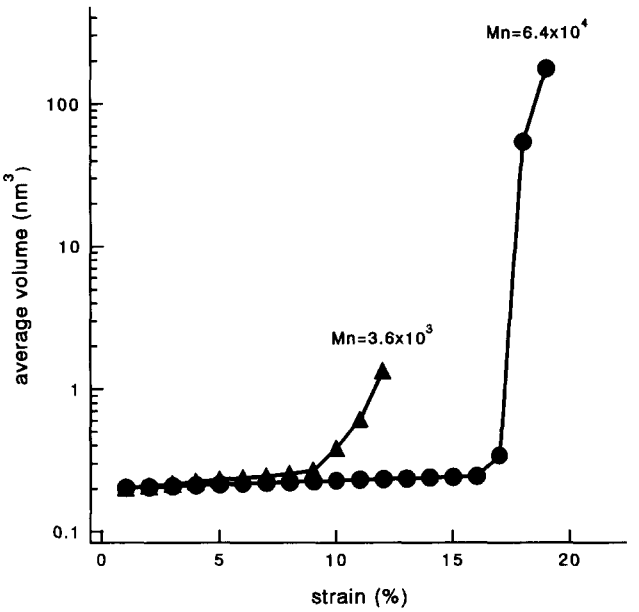

Figure 9 Calculated average volume of voids against the strain in polar model fibres with $M_n = 3.6 \times 10^3$ (▲) and $M_n = 6.4 \times 10^4$ (●)

interaction, and the stress on bonds or chains being more effectively transferred to others in polar models.

Our model initially contains numbers of defects due to chain-ends. The size of those can be thought as the volume of a unit rectangular lattice, $4.8 \times 4.0 \times 8.6 \text{Å}^3$. As the strain increases, these defects are expanded, new defects may be created by bond-cleavage, and/or they may meet each other to form a larger region. These regions cannot support stress. We call such a region a void and define it as a continuous region where stress is less than 10% of the stress on the fibre. We calculated the average size of voids during the simulation, and plotted these in *Figure 9*. In the low molecular weight case average void-volume first increased with larger rate than the overall elongation ratio, indicating the pores between chain-ends were more selectively expanded than chains. This means the stress on chains was not effectively transferred to other chains, and this is the reason that the slopes of the curves of lower molecular weight cases were reduced. At the strain of 9% (close to the critical point) average volume began to increase significantly. Considering that no bond-cleavage had occurred until this strain ratio, this is the direct observation of chain-slippage. Thus, the mechanism of the fracture for the low molecular weight case can be attributed to the beginning and the acceleration of chain-slippage caused by enhanced stress. In the high molecular weight case average void-volume increased with the same rate of elongation until the strain of 17%, then it increased rapidly. As shown in *Figure 6*, significant bond-cleavages began to occur at strains between 17% and 18%. The mechanism of the fracture in the high molecular weight case can be thought as the catastrophic bond-cleavage and rapid propagation of voids.

CONCLUSION

The model and method were developed to estimate the tenacity of perfectly oriented fibres of polymers of finite molecular weight. This model can also be applied to various polymers by modifying bonding or nonbonding interaction. The results were discussed in terms of the effect of molecular weight and nature of intermolecular interactions.

The tenacity of the model fibres was found to depend strongly on average molecular weight, and different fracture mechanisms were observed for lower and higher molecular weight cases. In the lower molecular weight cases, where interchain interaction is not strong, the fracture was governed by chain-slippage and assumed plastic behaviour. The tenacity is determined by the stress which causes chain-slippage, and the value can be thought to increase linearly with chain length. This should be the origin of the molecular weight dependence of the tenacity in this region. Therefore, the enhancement of the tenacity by polar interaction is more significant in the lower molecular weight cases. Conversely, in the higher molecular weight cases, where the interchain interaction is stronger than the bonds, the fracture was caused by the catastrophic bond-cleavages in the entire region of the fibre, and assumed brittle fracture. Here, the amount of defective regions, i.e. chain-ends and very short chains, must be important. The number of chain ends is inversely proportional to the average chain length. Therefore, the molecular weight dependence in the higher molecular weight cases differs from that in the lower molecular weight cases.

Our result for the nonpolar model is similar to that of Termonia *et al.*[4], except the tenacity calculated with our model is much larger. This is due to the different treatment of the van der Waals interaction. Because they treated the van der Waals interaction as a secondary bond active within a small distance, the magnitude of the interactions is smaller than ours. It is obvious that if one uses smaller interchain interaction in our model, the curves in *Figure 5* shift downward. The absolute value of the tenacity must be subject to the argument unless precise estimation of interchain interaction is possible. However, it is meaningful to discuss the general trend of the dependence of the tenacity and the fracture behaviour on the molecular weight and the nature of interchain interaction.

Finally, the tenacity estimated in our simulation, even for lower molecular weight, was higher than those reported for experimentally or commercially obtained high-strength fibres[13]. However, it is useless to arrange the parameters or potential functions in order to make the tenacity of the simulation comparable with experimental values because the structure and the mechanism of the fracture are totally different. In our models the structure of the fibres was mostly homogeneous except for chain-ends due to finite molecular weight, and the orientation of chains was perfect like a single extended crystal. Thus, the mechanism of the fracture was successfully described in terms of chain-slippage for the case of weaker interchain interaction and bond-cleavage for the case of stronger interchain interaction. In contrast, many types of inhomogeneity in the structure exist in real fibres such as extended crystals, lamellar crystals, taut tie molecules, relaxed molecules in amorphous phase etc.[14,15], and the fracture must be the result of the interrelated deformation of those elements. Even in the ultra-high strength polyethylene fibres, the fracture is determined by the defect region[16]. Therefore, it is not appropriate to compare our values directly with those of existing fibres. It should be emphasized that our methods

provide the tenacity that we can theoretically reach with polymers of finite molecular weight.

ACKNOWLEDGEMENT

We express many thanks to Professor K. Tashiro at Osaka University for the helpful suggestions.

REFERENCES

1 Ito, T. *Kagaku* 1982, **37**, 890
2 Boudreaux, D. S. *J. Polym. Sci., Polym. Phys. Edn.* 1973, **11** 1285
3 Crist, B. Jr. *J. Polym. Sci., Polym. Phys. Edn.* 1984, **22**, 881
4 Termonia, Y., Meakin, P. and Smith, P., *Macromolecules* 1985, **18**, 2246
5 Termonia, Y., Meaking, P. and Smith, P. *Macromolecules* 1986, **19**, 154
6 Termonia, Y. *J. Polym. Sci., Part B: Polym. Phys.* 1995, **33**, 147
7 Holmes, D. R., Bunn, C. W. and Smith, D. J., *J. Polym. Sci.*, 1955, **17**, 159
8 Pauling, L. 'The Nature of the Chemical Bond', 3rd Edn, Cornel Univ. Press, New York, 1960
9 Miyasaka, K., Isomoto, T. and Koganeya, H. *J. Polym. Sci., Polym. Phys. Edn.* 1980, **18**, 1047
10 Zhurkov, S. N. and Korsukov, V. E. *J. Polym. Sci., Polym. Phys. Edn.* 1974, **12**, 385
11 Mayo, S. L., Olafson, B. D. and Goddard III, W. A. *J. Phys. Chem.* 1990, **94**, 8897
12 'Annual Book of ASTM Standards', Vol. 07.01m ASTM, PA, 1991, p. 450
13 Ohta, T. *Polym. Eng. Sci.* 1983, **23**, 697
14 Perterlin, A. *J. Polym. Sci. (A2)* 1969, **7**, 1151
15 Bashir, Z., Odell, J. A. and Keller, A. *J. Mater. Sci.* 1984, **19**, 3713
16 Smook, J., Hamersma, W. and Pennings, A. J. *J. Mater. Sci.* 1984, **19**, 1359